Oncogene (2002) 21, 4462–4470

www.nature.com/onc

Allelic loss and reduced expression of the *ING3*, a candidate tumor suppressor gene at 7q31, in human head and neck cancers

Mehmet Gunduz[1,3], Mamoru Ouchida[2], Kunihiro Fukushima[1], Sachio Ito[2], Yoshimi Jitsumori[2], Tomoko Nakashima[1], Noriyuki Nagai[3], Kazunori Nishizaki[1] and Kenji Shimizu*[,2]

[1]Department of Otolaryngology, Graduate School of Medicine and Dentistry, Okayama University, Shikata 2-5-1, Okayama 700-8558, Japan; [2]Department of Molecular Genetics, Graduate School of Medicine and Dentistry, Okayama University, Shikata 2-5-1, Okayama 700-8558, Japan; [3]Department of Oral Pathology, Graduate School of Medicine and Dentistry, Okayama University, Shikata 2-5-1, Okayama 700-8558, Japan

Loss of heterozygosity (LOH) has been frequently detected at chromosome 7q31 region in human head and neck squamous cell carcinomas (HNSCC) and many other cancers, suggesting the existence of tumor suppressor genes (TSG). We analysed LOH at 7q31 region in 49 HNSCC by using six polymorphic microsatellite markers and found allelic deletion in 48% (22/46) of the informative cases. We detected two preferentially deleted regions, one is around D7S643 and the other around D7S486. When we redefined the map of 7q31 region according to the contiguous sequences, a recently identified gene, *ING3*, was found in the proximity of D7S643. ING3 protein harbors the PHD domain highly homologous among ING family proteins, in which we previously found mutations in a related gene, *ING1*. As only one missense mutation of the *ING3* gene was found in HNSCC, we examined the expression level. Reverse-transcription-PCR analysis demonstrated decreased or no expression of ING3 mRNA in 50% of primary tumors as compared with that of matched normal samples. Especially, about 63% of tongue and larynx tumors showed the decrease and a tendency of higher mortality was observed in cases with decreased ING3 expression. All these findings suggest a possibility that the *ING3* gene functions as a TSG in a subset of HNSCC.
Oncogene (2002) **21,** 4462–4470. doi:10.1038/sj.onc.1205540

Keywords: loss of heterozygosity; *ING3*; tumor suppressor gene; reduced expression; ING family; head and neck cancer

Introduction

Tumor suppressor genes (TSG) are defined as genetic elements whose loss or mutational inactivation allows cells to acquire neoplastic growth (Hinds and Weinberg, 1994). Cytogenetic studies have shown frequent chromosome 7 abnormalities in human head and neck squamous cell carcinomas (HNSCC) (Cowan *et al*., 1992). Microcell-mediated transfer of human chromosome 7 into a murine squamous cell carcinoma cell line (Zenklusen *et al*., 1994), or into a highly aggressive human prostate carcinoma cell line (Zenklusen *et al*., 2000), inhibited the tumorigenicity of these cell lines. Similarly, insertion of an intact human chromosome 7 into an immortalized human fibroblast cell line with 7q31-32 deletion suppressed the immortality of the cells and restored their ability to senescence (Ogata *et al*., 1993). All these studies provided some clues for the existence of a TSG(s) or a senescence-related gene(s) on chromosome 7.

Loss of heterozygosity (LOH) analysis by using polymorphic microsatellite markers is a sensitive method to detect micro-deletions. Frequent LOH in a chromosomal region is considered as an indication of the presence of a putative TSG (Knudson, 1993; Lin *et al*., 1996). Recent studies have shown the frequent LOH at chromosomal region 7q31 in HNSCC (Zenklusen *et al*., 1995; Wang *et al*., 1998), and also in various types of human cancers including breast, prostate, colon, ovary, thyroid and renal cell carcinomas (Latil *et al*., 1995; Takahashi *et al*., 1995; Zenklusen *et al*., 1995; Lin *et al*., 1996; Shridhar *et al*., 1997; Bieche *et al*., 1997; Zhang *et al*., 1998; Edelson *et al*., 1997). In this study, we examined the 7q22-31 region by using a set of highly polymorphic microsatellite markers to find out allelic loss in HNSCC. In the light of LOH analysis, we redefined the map of chromosome 7q31 region and examined some genes on this region by analysing mutation and mRNA expression. The results suggested that the *ING3* gene is a likely candidate for one of the TSGs at 7q31. The prototype of the *ING* family gene, *ING1*, has been inferred for possible TSG function (Garkavtsev *et al*., 1996) and we have recently found allelic loss and tumor-specific mutations of the gene in HNSCC (Gunduz *et al*., 2000).

*Correspondence: K Shimizu;
E-mail: shimke47@md.okayama-u.ac.jp
Received 15 August 2001; revised 18 March 2002; accepted 27 March 2002

Results

LOH analysis

We examined LOH using six microsatellite markers on the chromosome 7q22-31 region in 49 paired normal and HNSCC DNAs. Overall, 48% (22/46) samples showed LOH at least one marker on 7q31. Figure 1a summarizes the results of LOH analyses. We detected two distinct regions of deletion. Markers D7S643 and D7S486 showed the highest incidence of LOH with a value of 35%, while flanking markers demonstrated lower frequency. Five tumors (samples 18, 24, 34, 38 and 49) showed a deletion around the marker D7S643, while five tumors (samples 8, 20, 21, 23 and 41) displayed a deletion preferentially around the marker D7S486. Seven tumors (samples 16, 26, 32, 39, 43, 47 and 48) demonstrated comparatively wide deletion including both of the above markers. Interestingly, three tumors (samples 7, 37 and 45) showed deletions around both markers D7S643 and D7S486 in spite of retaining another marker D7S522, which locates in

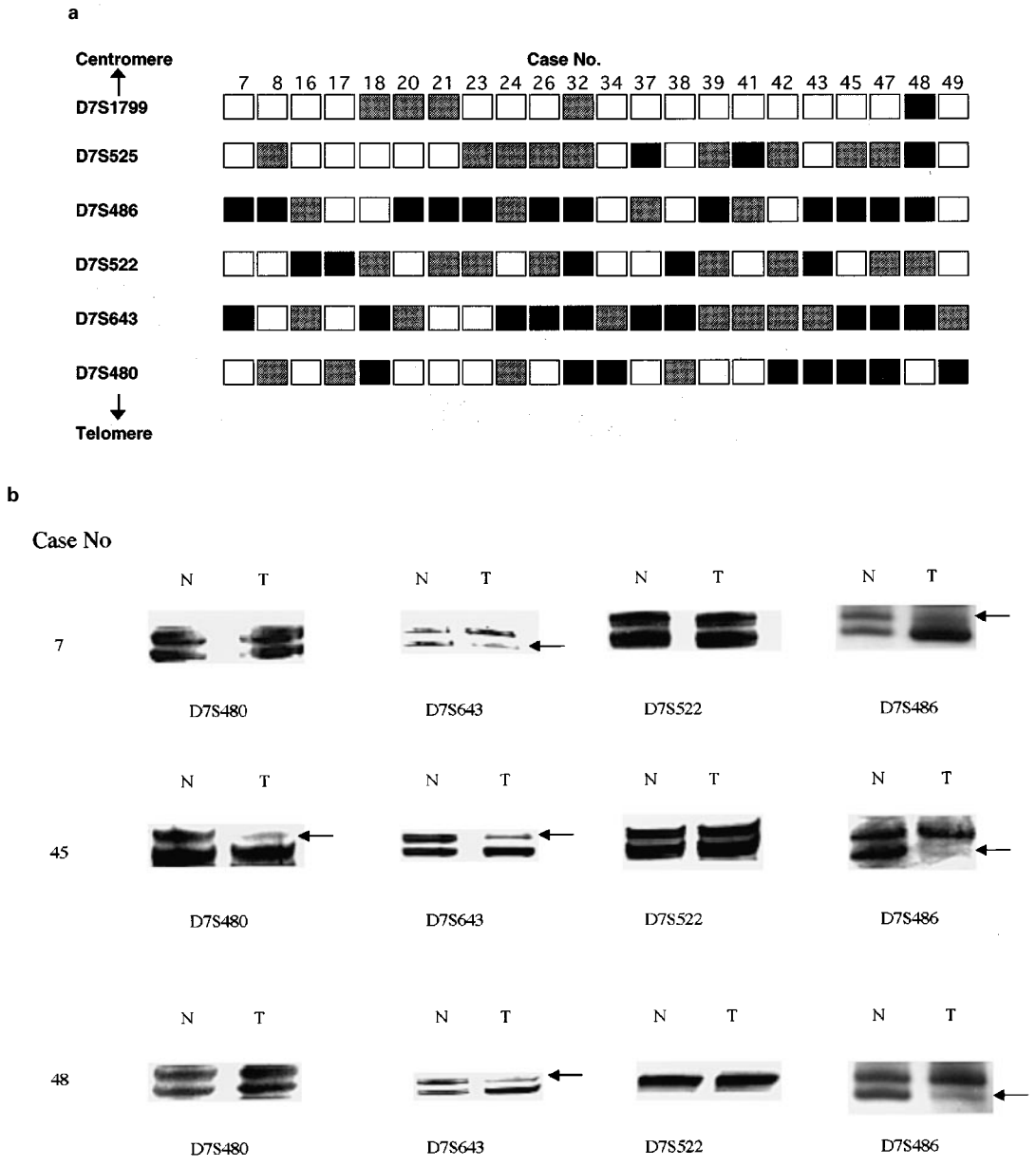

Figure 1 LOH analysis on chromosome 7q31 in HNSCC. (**a**) Schematic representation of LOH distribution. Case numbers are shown at the top. Microsatellite markers used are shown to the left. Filled box, LOH; open box, retention of heterozygosity; shaded box, not informative (homozygous). (**b**) Primary LOH data from three representative HNSCC. Case numbers are shown at the left. N, normal DNA; T, tumor DNA. Lost alleles are shown by arrows

between the former two markers. These results indicated that two different deleted regions were mapped to the vicinity of the markers D7S643 and D7S486, respectively. Representative examples of LOH are shown in Figure 1b.

Mapping of chromosome 7q31 region

Most of the chromosome 7 region has been sequenced and contiguous sequence results are available through the genome database on National Human Genome Research Institute home page (http://genome.nhgri.nih.gov/chr7/). We searched the database and redefined the map of this region including the microsatellite markers that we used for LOH analysis as shown in Figure 2. Our data pointed out a region around marker D7S643 as one of hot locations for TSG. The *ING3* gene, a novel member of the *ING* family, of which

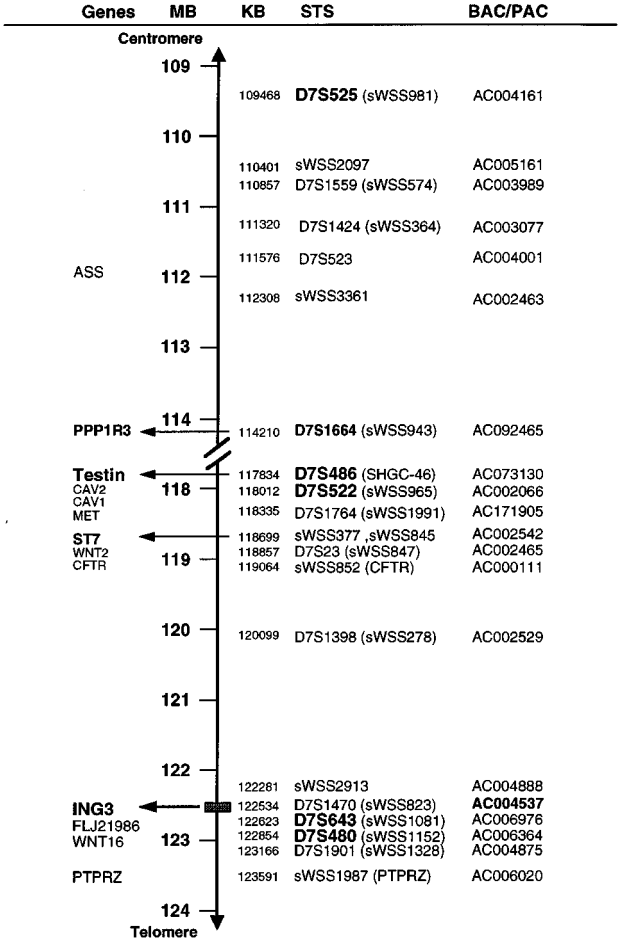

Figure 2 A physical map of the D7S525 - D7S480 genomic interval. Most of the markers, BAC and PAC clones shown were derived from the National Human Genome Research Institute (http://genome.nhgri.nih.gov/chr7/), National Center for Biotechnology Information (NCBI) (http://www.ncbi.nlm.nih.gov/) and the Genome Database (http://gdbwww.gdb.org/). The order of markers presented here is based upon the latest mapping information of these sites and is tentative

cDNA sequence was recently identified but yet published (GeneBank accession number: AF074968 and NM_019071, with an annotation made by Kawabata *et al*.) was found to be very close to the marker D7S643. The *ING3* gene resides within 100 kbp to the marker D7S643, and it seemed that no other candidate TSG exists in this region.

Characterization of the human ING3 *gene*

One PAC clone (GeneBank accession number: AC004537) included the genomic DNA covering the entire region of the *ING3* gene. When the amino acid sequence of the *ING3* gene product, a putative 47 kDa protein (418 amino acids), was aligned with other four members of ING family proteins so far known, ING3 showed high homology with other members especially within PHD zinc finger domain and weak homology over the whole sequence particularly with ING1-p47 (Figure 3). Of these sequences, only ING1 and ING2 (ING1L) were published (Garkavtsev *et al*., 1996; Shimada *et al*., 1998; Nagashima *et al*., 2001). As some tumor specific mutations we previously reported are located in the PHD domain of ING1 protein (Gunduz *et al*., 2000), the potential important role of PHD domain has to be noticed commonly on the ING family proteins. The *ING3* gene was composed of at least 12 exons spanning over 25 kb genomic interval (Figure 4a). To analyse the promoter for the *ING3* gene, the 5′ flanking 1.5 kb region including 5′-noncoding region of exon 1 was subcloned in sense or antisense orientation (Figure 4b). Luciferase construct in sense orientation showed about 213-fold increase in luciferase activity as compared with the promoterless luciferase plasmid, while activity of luciferase construct in antisense orientation was not detectable. We searched for binding sites for transcription factors on this 1.5 kb promoter region, and found some binding motifs for factors such as Oct1, STAT, CREB and E2F (Figure 4b).

As revealed by Northern blot analysis (Figure 4c), about 1.9 kb of ING3 transcript was detected in human heart, skeletal muscle, thymus, spleen, kidney, liver, placenta and peripheral blood leukocytes. ING3 mRNA expression in brain, colon, small intestine and lung was below the detectable level. We also found an alternatively spliced form of the ING3 message by cDNA cloning from human normal tissues. This variant form was devoid of the exon 3 but the coding frame was not shifted (data not shown).

Mutation analysis

We examined all exons of the *ING3* gene for mutation analysis by PCR-SSCP (single-strand DNA conformational polymorphism) and direct sequencing in 49 HNSCC and four tumor-derived cell lines. We detected a tumor specific missense mutation in one sample and a silent change in three samples (data not shown). Sample 41 demonstrated a nucleotide change from GAC to GGC at codon 20 with an amino acid

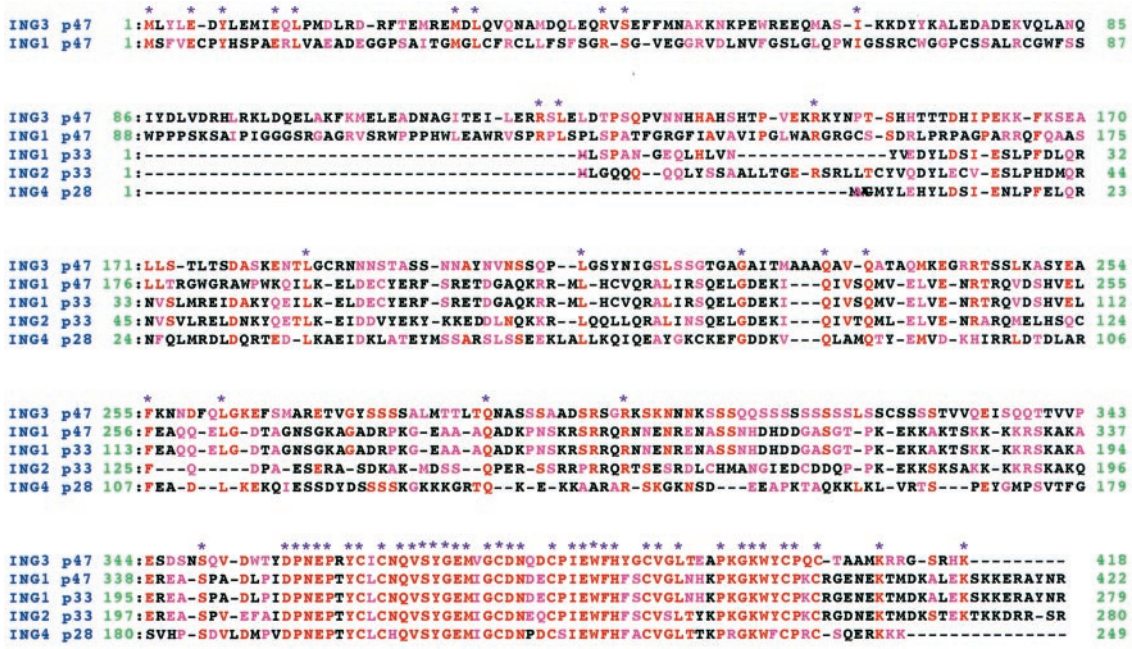

Figure 3 Alignment of amino acid sequences of the ING family proteins. Identical amino acids with ING3 protein are indicated by red and similar residues by purple. Asterisks above denote residues perfectly conserved among the family members. GenBankPep Accession number for each protein sequence is following; ING3 (NP_061944), ING1-p47 (BAB08102), ING1-p33 (BAB08101), ING2 (NP_001555), ING4 (NP_057246, another name, LOC51147 of which annotation was made by Peng *et al*. in the protein data base of NCBI)

substitution from aspartic acid to glycine. Samples 19, 36 and 47 showed a silent mutation from GAC to GAT at codon 356 without an amino acid change. Since normal samples corresponding to these tumors also showed the same silent change, this was considered as a polymorphism.

ING3 mRNA expression analysis

Since mutation in this gene was very rare, we looked for other possible inactivation mechanisms. For this aim, we analysed the expression level of ING3 mRNA in tumor samples comparing with the paired normal tissue. In 40 available matched RNA samples, the expression levels of ING3 mRNA were compared by quantitative RT–PCR using glyceraldehyde phosphate dehydrogenase (GAPDH) mRNA as a control (Figure 5 and Table 1). PCR primers were designed to encompass the exon/intron junctions on the cDNA in order to eliminate the potential contamination of genomic DNA. Twenty out of 40 tumor tissues (50%) showed decreased or no expression of ING3 mRNA as compared with that of each paired normal tissue, while 38% (15/40) of samples showed similar level of the expression in normal and tumor tissues. In 12% (5/40) of samples, increased expression of ING3 was detected in tumor tissues. One of the five tumors had the missense mutation at the codon 20. We compared the expression levels in HNSCC-derived cell lines by using the average value of ING3 mRNA in normal tissue samples. The expression level was decreased in three cell lines (T3M-1, SCC-KN and SCC-TF). One cell line (HSQ-89) exhibited a tendency toward the lowered expression.

Relationship between ING3 expression and clinicopathological parameters

Examination of the relationship between ING3 mRNA expression levels and clinicopathological features such as stage, differentiation, recurrence, distant metastasis, lymph node metastasis and survival did not indicate any significant correlation (data not shown). However, we noticed a locational preference of decreased ING3-expression in some tumor types. About 64% of the tongue and 63% of the larynx tumors showed decreased expression in tumor samples as compared with that of paired normal tissues, while it was only 17 and 20% for hypopharynx and oropharynx cancer samples, respectively. Long term follow up was available for 32 patients. Kaplan–Meier test showed a tendency of high mortality in cases who had tumors with decreased ING3 mRNA expression compared to cases with tumors showing normal or high ING3 expression (data not shown), though the statistic significance was very low ($P=0.46$). Nevertheless, the mean survival period of the group with decreased ING3 expression was about 10 months shorter than that of the group with normal or increased expression (data not shown).

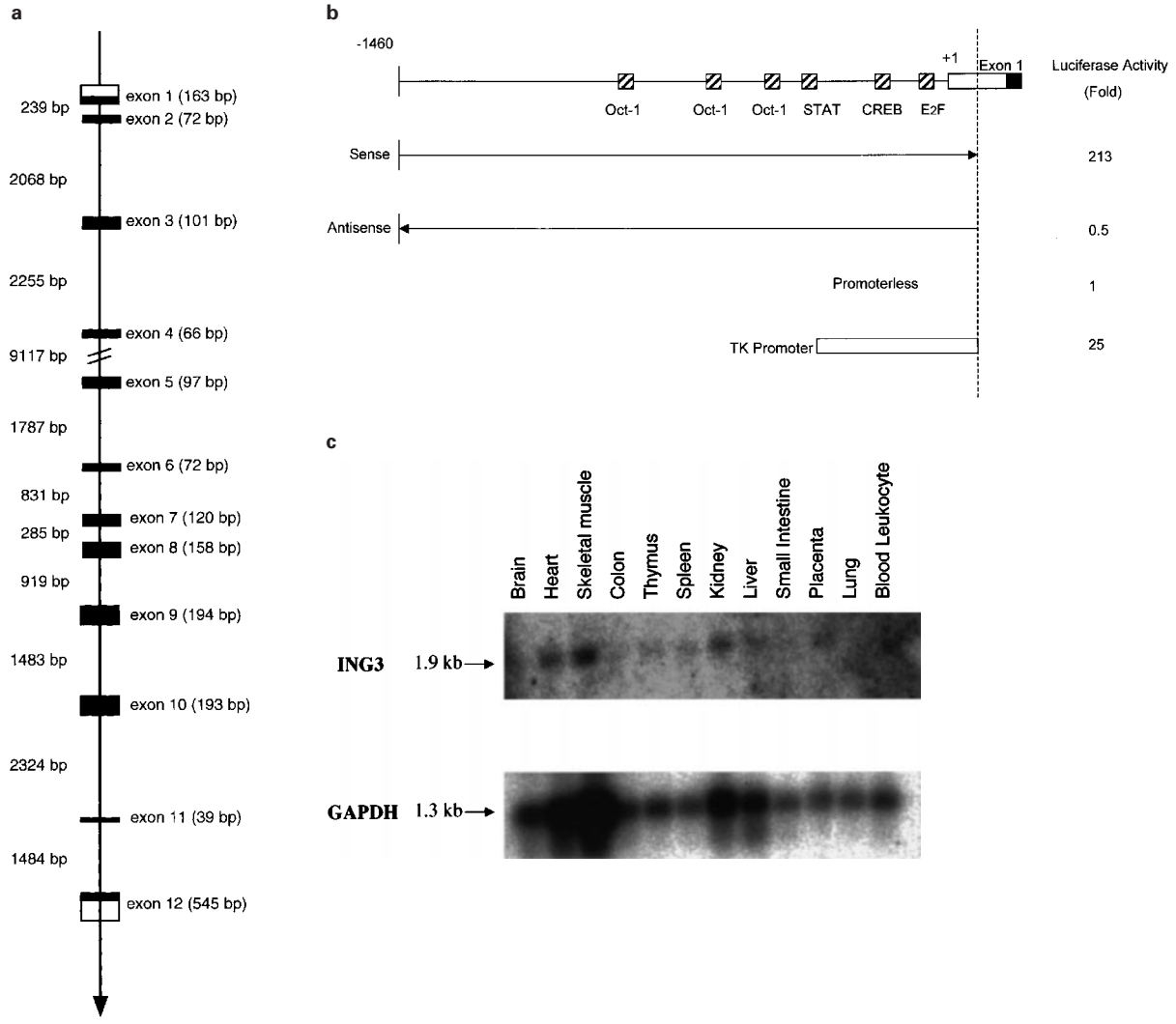

Figure 4 Characterization of the *ING3* gene. (**a**) Genomic structure of the *ING3* gene. The gene has 12 exons spanning over 25 kb genomic interval. (**b**) Luciferase analysis of the *ING3* promoter. The 5′ flanking 1460 bp region including a part of exon 1 was used for the luciferase assay. The luciferase activity measured with 293 cells are shown to the right as compared with that of the promoterless reporter plasmid. Filled box, coding region in exon; open box, noncoding region in exon; Putative binding sites for some transcriptional factors are indicated on the promoter region as shaded boxes. (**c**) Northern blot analysis of ING3 mRNA. An 1.9 kb of ING3 transcript was detected in various human tissues. Sources of mRNA in the lanes are indicated at the top. GAPDH mRNA of about 1.3 kb was used as an internal control

Discussion

We examined LOH at chromosome 7q22-31 region in 49 HNSCC by using six microsatellite markers. We found the deletions at 7q31 in almost half of the HNSCC samples (48%), while this value was lower than those of two previous reports in HNSCC with 56% and 67% LOH, respectively (Zenklusen *et al*., 1995; Wang *et al*., 1998), probably because the specimens we used were not micro-dissected. In this study, however, we detected two distinct deletion regions around the markers D7S643 and D7S486, which is telomeric and centromeric to the marker D7S522, respectively. Although most tumors showed a comparatively wide deletion from D7S643 to D7S486, three tumors demonstrated two different deleted regions around the markers D7S643 and D7S486 but retaining an intact region between them. This suggests that there may be two different TSGs for HNSCC in this region. The region of 7q31, including D7S486 to D7S480 markers, has been focused as a hot location for LOH in many types of human cancer (Zenklusen *et al*., 1995; Wang *et al*., 1998; Latil *et al*., 1995; Takahashi *et al*., 1995; Bieche *et al*., 1997). Edelson *et al*. (1997) reported two different regions with high incidence of LOH, one was around D7S643 and the other around D7S522 in ovarian cancers, similar to our results. Thus, deletions at 7q31 region appear to be

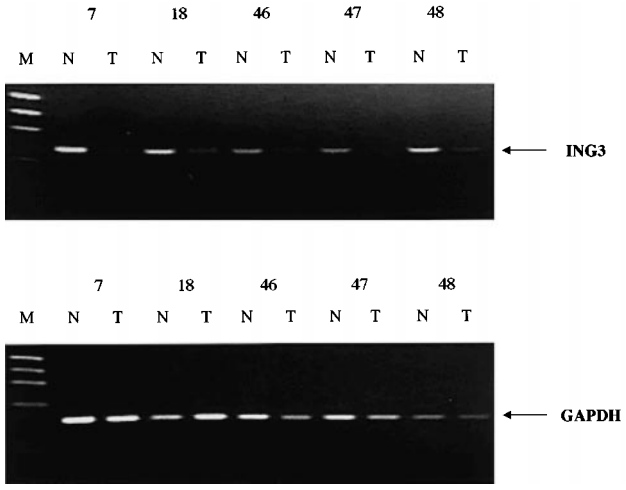

Figure 5 ING3 expression analysis in matched tumor and normal samples. Representative raw data of RT–PCR are shown; Upper band, ING3 message (703 bp); Lower band, GAPDH message (456 bp); N, non-tumor tissue; T, tumor tissue; M, size marker. Upper numbers in each figure (7, 18, 46, 47 and 48) show case numbers

Table 1 Quantitation of ING3 mRNA in HNSCC and tumor-derived cell lines

Case no.	*Ratio*	*Class*	*Case no.*	*Ratio*	*Class*
1	1.57	H	28	0.56	L
5	0.40	L	29	1.10	N
6	1.35	N	30	0.58	L
7	No expr.	L	33	0.72	N
8	0.64	N	34	1.20	N
9	0.46	L	35	0.33	L
10	0.40	L	36	0.50	L
11	2.00	H	39	1.30	N
12	0.68	N	40	0.31	L
13	1.00	N	41	1.80	H
15	1.00	N	42	1.90	H
16	1.30	N	43	1.37	N
17	0.48	L	44	2.50	H
18	0.37	L	45	1.22	N
19	0.55	L	46	0.23	L
20	1.00	N	47	No expr.	L
21	0.52	L	48	0.17	L
22	0.34	L	49	0.38	L
23	0.16	L	SCC-TF	0.23	L
25	0.47	L	SCC-KN	0.38	L
26	1.00	N	HSQ-89	0.63	N
27	1.17	N	T3M1	0.16	L

The ratio of the expression levels in the matched tumor and normal samples was calculated as described in Materials and methods. Decreased and increased expression levels were shown as classes L and H when this ratio was less than 0.6 and greater than 1.4, respectively. Class N means the value of ratio between 0.6 and 1.4. 'No expr.' means no expression of ING3 mRNA

very common in various cancers suggesting the presence of either a cluster of TSGs, each of which is involved in one tumor type, or a few TSGs involved in the etiology of many tumor types.

Based on the recent human genome information, we redefined this region and mapped the *ING3* gene, a novel member of the *ING* family, within one of the two peak areas of LOH we found. We therefore examined mutations in all exons of the *ING3* gene in 49 HNSCC samples to investigate whether it is the target of functional loss in tumors. One tumor-specific missense mutation and three silent changes were detected. This missense mutation caused an amino acid change from aspartic acid to glycine at the N-terminal portion of ING3 protein. Although we do not know the importance of this mutation yet, it may exert an important change in structure and function of the protein.

Since *ING3* mutation was very rare in our study, there may be other inactivation mechanisms. In facts, analyses of ING3 mRNA showed the decreased expression in 50% of primary tumors and 75% of tumor derived cell lines. Particularly, two primary tumors exhibited complete loss of the ING3 mRNA expression. Many of the other tumor samples showed less than half level of mRNA expression as compared with that of normal samples, though the expression level in tumor was not completely associated with LOH.

We could not find any significant correlation between clinicopathological features and expression levels of the *ING3* gene except for tumor location. Majority of tongue and larynx cancers displayed decreased ING3 expression while only a small subset of oropharynx and hypopharynx cancers showed a decrease. We noticed a tendency toward earlier death in patients with tumor showing lower ING3 mRNA expression. This result suggests the potential prognostic significance of the *ING3* gene and also supports the possible tumor suppressor character of the gene. Further analysis with more samples at different locations may make this point clear.

Rare mutation but a considerably decreased expression of the *ING3* gene suggests that the down-regulation of this gene by transcriptional mechanism, such as promoter methylation, is an important step for carcinogenesis. We recently reported a high incidence of LOH and tumor-specific somatic mutations of the *ING1* gene located on chromosome 13q34. One *ING1* allele was deleted in 49% of HNSCC, although the incidence of the *ING1* mutation was only 13% in HNSCC (Gunduz *et al*., 2000).

ING proteins belong to a family of proteins containing the plant homeodomain (PHD) finger, which includes transcription factors and proteins that regulate chromatin structure. Although the exact mode of action of ING proteins is yet to be known, several reports suggested that ING proteins may affect the activity of p53. ING1 proteins have at least four splicing variants (Gunduz *et al*., 2000) and one of the variants, which is physically associated with p53, inhibits cell cycle progression (Garkavtsev *et al*., 1998). ING2 protein negatively regulates cell proliferation and survival in a p53-dependent manner through induction of the G1 phase cell-cycle arrest and

apoptosis (Nagashima *et al*., 2001). Furthermore, ING1 and ING2 proteins are associated with histone acetyltransferase activities (Loewith *et al*., 2000; Nagashima *et al*., 2001). Actually, one of the spliced forms of ING1 is functionally associated with histone deacetylase (HDAC)-dependent transcriptional repression, in reporter gene expression assays *in vivo*, and in histone deacetylation assays *in vitro* (Skowyra *et al*., 2001). Moreover, recent analysis of mouse *Ing1* gene on structure and function suggested that a smaller isoform of ING1 protein, the mouse equivalent of human p24ING1c, is required for the activation of p53-responsive genes, in contrast, overexpression of the larger form, an equivalent of the human p33ING1b protein, interferes the activation of p53-dependent promoters when p53 is stabilized after DNA damage (Zeremski *et al*., 1999). In fact, our analysis of ING1 mRNA expression demonstrated that one of the spliced form (p24ING1c) was reduced in most tumor tissues, while the other major variant (p33ING1b) showed variable expression in different tumors. However, when the expression of p33ING1b was reduced, p24ING1c was almost always decreased (Gunduz *et al*., unpublished data). Toyama *et al*. (1999) reported that the *ING1* gene showed decreased expression in 44% of tumors compared with matched normal samples, while 23% of tumors demonstrated increased expression in 377 primary breast cancers, although only one germ line missense mutation was found. It seems likely that isoforms of ING1 protein as well as different members of the ING family proteins may have different roles in growth control and that their unique N-terminal sequences may be implicated in the difference. Thus, the inter-relationship among ING family proteins are complicated and may affect the expression of each other. Further functional studies are warranted to elucidate the exact relationship among ING family members and their individual and combined effects on cell growth. We compared the LOH status at both *ING1* and *ING3* loci in each HNSCC specimen. Interestingly, 73% of informative cases with LOH at the *ING1* region also showed deletion at the *ING3* region (data not shown). Concomitant deletion of both of the two genes in many HNSCC samples may lead to the haploid insufficiency in respect to the levels of ING family proteins even without inactivating mutations or gene silencing.

So far, some genes were proposed as candidate TSGs at 7q31 region. Hurlstone *et al*. (1999) reported mapping of the *Caveolin-1* gene, a membrane-bound signaling mediator (Wary *et al*., 1996), in the proximity of the marker D7S522 on 7q31. However, they found neither mutations nor methylation at the promoter region of the *Caveolin-1* gene in both primary cancers and tumor cell lines. Genetic alterations of the *PPP1R3* gene, encoding the regulatory subunit 3 of protein phosphatase 1 located at 7q31, have been reported in nine cell lines from various types of human cancers (Kohno *et al*., 1999). Therefore, *PPP1R3* has been considered as a candidate TSG in this region. However, when we determined the precise map position of the *PPP1R3* gene, the BAC clone harboring the gene was located about 4 MB apart from the marker D7S486 (Figure 2), which may be outside the consensus LOH area in HNSCC.

A recently identified gene, *TESTIN*, was proposed as a candidate TSG at 7q31 region (Tatarelli *et al*., 2000). They detected three missense mutations of the gene. Lack of expression was observed in 22% of cancer cell lines and 44% of cell lines derived from hematological malignancies, while TESTIN mRNA was expressed in all normal tissues. As D7S486 marker is located in the intron 6 of this gene, the targeted gene in the LOH area around D7S486 detected in our study may correspond to the *TESTIN* gene. Another novel TSG candidate gene, *ST7*, has recently been identified at 7q31.1 (Zenklusen *et al*., 2001). Six mutations of the gene were found in breast tumors and primary colon carcinomas. Sequence-based mapping of the *ST7* gene revealed that the gene resides in between the markers D7S522 and D7S643, but much closer to the former (Figure 2). Since the incidence of LOH at D7S522 was significantly lower than that at D7S643 in HNSCC (Figure 1a), we suppose that the *ST7* does not play an important role in the development of HNSCC.

Finally, our study suggested the *ING3* gene as a candidate TSG at 7q31 region with considerable supporting findings at least in cases of HNSCC. In the light of this study and previous reports, further works on these candidate genes with more samples of various types of human cancers are required to elucidate their roles in human carcinogenesis.

Materials and methods

Tissue samples

Paired normal and tumor samples were obtained from 49 patients with primary HNSCC at the Department of Otolaryngology Okayama University Hospital after acquisition of written informed consent from each patient. All tissues were frozen in liquid nitrogen immediately after surgery and stored at $-80^{\circ}C$ until the extraction of DNA and RNA.

Cell lines

HNSCC cell lines, SCC-KN and SCC-TF, derived from tongue tumor, T3M-1, derived from oral cavity tumor and HSQ-89, derived from maxillary sinus tumor, were purchased from Riken cell bank (Tsukuba, Japan).

DNA and RNA extraction

Genomic DNAs were isolated from frozen tissues by SDS/proteinase K treatment, phenol-chloroform extraction, and ethanol precipitation. Total RNAs were prepared by using a modified acid guanidinium phenol chloroform method (ISOGEN; Nippon Gene Co., Tokyo, Japan).

Microsatellite analysis

Primers for amplification of microsatellite markers D7S480, D7S643, D7S522, D7S486, D7S525 and D7S1799 are available through the internet genome database (http://gdbwww.gdb.org/). PCR amplification was carried out in 20 μl of reaction mixture as described (Gunduz *et al*., 2000). Initial denaturation at 94°C for 3 min was followed by 25 cycles of a denaturation step at 94°C for 30 s, an annealing step at 54°C (D7S1799, D7S525 and D7S486) or 60°C (D7S522, D7S643 and D7S480) for 30 s, and an extension step at 72°C for 1 min. A final extension step at 72°C for 7 min was added. After amplification, 2 μl of the reaction mixture was electrophoresed through an 8% polyacrylamide gel containing 8 M urea. The DNA bands were visualized by silver staining (Bassam *et al*., 1991). LOH was scored if one of the heterozygous alleles showed at least 50% reduced intensity in tumor DNA as compared with that of the corresponding normal DNA.

RT–PCR analysis

Total RNA was reverse-transcribed with the SuperScript Preamplification System (Gibco BRL, Grand Island, NY, USA) starting with 3 μg of total RNA from each sample, according to the procedures provided by the supplier. One μl of each RT reaction was amplified in 50 μl mixture containing 1.2 mM $MgCl_2$, 1 × PCR buffer, 200 μM of each deoxyribonucleoside triphosphate (dNTP), 20 pmol of each primer, and 1 unit of rTth DNA polymerase XL (Applied Biosystems, Foster City, CA, USA). Thirty-five PCR cycles for ING3 primers, S2 [5′-CAGCCTCTTCTAACAATGCCTA] and RAS1 [5′-CTTCATCAAACAAAAGGACCACC], and 25 cycles for GAPDH primers, S1 [5′-AGACCACAGTCCATGCCATCAC] and AS1 [5′-GGTCCACCACCCTGTTGCTGT], were used for amplification. Appropriate cycling number for non-saturating measure was determined empirically by a quantitative PCR system (ABI GeneAmp 5700, Applied Biosystems). PCR amplification was done essentially as described in microsatellite analysis, except that the annealing step was at 60°C for 1 min.

Quantitation of the RT–PCR products

PCR products were separated through 2% agarose gel and stained with ethidium bromide. The size of the PCR products was 456 bp for GAPDH and 703 bp for ING3. The intensity of ethidium bromide staining of each band was measured by a CCD image sensor (Gel Print 2000/VGA, Toyobo, Osaka, Japan), and analysed by a computer program for band quantification (Quantity One, Toyobo). The value of tumor-specific ING3 expression was determined by calculating the ratio of the expression level in the tumor and that in the matched normal sample, each of which was normalized for the corresponding GAPDH expression level. Decreased and increased expression levels were defined when this ratio was less than 0.6 and greater than 1.4, respectively. Reproducibility was confirmed by independent PCR repeated twice.

Luciferase assay

Putative promoter region including the 5′-noncoding region of exon 1 was inserted in the promoterless luciferase plasmid pOA-luciferase (Kukita *et al*., 1999) in either sense or antisense orientation to produce reporter plasmids for the luciferase assay. Each reporter plasmid (0.5 μg) was cotransfected with 0.25 μg of an internal control Renilla luciferase plasmid, pRL-TK (Promega, Madison, WI, USA), into 293 human embryonic kidney cells using the calcium phosphate coprecipitation method. Cells were harvested 48 h after transfection. The activities of firefly and Renilla luciferase were measured simultaneously using the Dual-Luciferase Reporter Assay kit (Promega) and normalized for the variation in transfection efficiency. These assays were repeated twice in duplicate.

Northern blot analysis

Northern blot analysis was done according to the standard procedure (Tanino *et al*., 1999) on a nylon membrane with 2 μg of poly(A^+) mRNA (human MTN blot; Clontech) using α-^{32}P-dCTP-labeled ING3 cDNA as a probe. After hybridization, the filter was exposed to an imaging plate for image analyser BAS2000 (Fuji Film, Tokyo, Japan). The filter was rehybridized with another probe for GAPDH as an internal control.

PCR–SSCP analysis

Each of the coding region of exon 1 to 12 was amplified by PCR with intron spanning primers for exon 1, RS1 (5′-GCGATGTTGTACCTAGAAGACT) and EX2-AS (5′-GGAGTAGTAGACGCGCCGAC), for exon 2, EX2-S (5′-GCCCCTCTGACGGACTCTC) and EX2-AS (5′-GGAGTAGTAGACGCGCCGAC), for exon 3, EX3-S (5′-CCCTCCCTAAATCAAACCATGT) and EX3-AS (5′-GATAAATTATCCAAAGTGTTGCAC), for exon 4, EX4-S (5′-GCAGTTGTATGTCCTGCATATGA) and EX4-AS (5′-CACAGTATGCACATTACTTTTACT), for exon 5, EX5-S (5′- AGCTGACACTTTAACAGTGTCC) and EX5-AS (5′-AGCGATTTGCACATGTACTGTC), for exon 6, EX6-S (5′-TGTATCTCTGTGCCTCTCTTCT) and EX6-AS (5′-CTTAGCTGCACTACACCAAACT), for exon 7, EX7-S (5′-TGCCTTGTCCATAGTTCTCTAAA) and EX7-AS (5′-CTAACACAAACAAACAAAGCAATC), for exon 8, EX8-S (5′-GTTCTCTGCAACCATTTTTATTTC) and EX8-AS (5′-GTAACATTTTGTCTCTAAACCCT), for exon 9, EX9-S (5′-TGATGCTATCAATGAATGTCTATT) and EX9-AS (5′-AGTAAAGGTATAGGGCTACTGT), for exon 10, EX10-S (5′-AACTTCTGGATGGTGAGCAAATA) and EX10AS2 (5′-GAAATAGTTCTCTTCCTTCTAGT), for exon 11, EX11-S (5′-GTTAATTGGTATCTAGGTGTTTGT) and EX11-AS2 (5′-CTTAGACCAAACCATACAGCAA), for exon 12, EX12-S (5′-TTGCAATTTTGCTTTCTAGTGCC) and RAS1 (5′-CTTCATCAAACAAAAGGACCACC). PCR amplification, SSCP analysis, reamplification of the altered fragments, and sequencing analyses were done as described (Gunduz *et al*., 2000).

Statistic analysis

Student's *t*-test and χ^2 test were performed to estimate the correlation between the ING3 mRNA expression levels and clinicopathological factors. Kaplan–Meier plot with the log-rank test was used for survival analysis.

Acknowledgments
We would like to thank cell depositors, Drs M Urade, T Okabe and M Miyake for their kind approval for the cell distribution through cell bank. We thank T Fujiwara, A Sakai and H Hanafusa for technical support and the surgeons in the Department of Otolaryngology of our

Medical School for providing fresh specimens. This work was supported by grants-in-aids from the Ministry of Education, Science, Sports and Culture and from the Ministry of Health and Welfare of Japan to K Shimizu.

References

Bassam BJ, Caetano-Anolles G and Gresshoff PM. (1991). *Anal. Biochem.,* **196,** 80–83.

Bieche I, Khodja A, Driouch K and Lidereau R. (1997). *Clin. Cancer Res.,* **3,** 1009–1016.

Cowan JM, Beckett MA, Ahmed-Swan S and Weichselbaum RR. (1992). *J. Natl. Cancer Inst.,* **84,** 793–797.

Edelson MI, Scherer SW, Tsui LC, Welch WR, Bell DA, Berkowitz RS and Mok SC. (1997). *Oncogene,* **14,** 2979–2984.

Garkavtsev I, Kazarov A, Gudkov A and Riabowol K. (1996). *Nat. Genet.,* **14,** 415–420.

Garkavtsev I, Grigorian IA, Ossovskaya VS, Chernov MV, Chumakov PM and Gudkov AV. (1998). *Nature,* **391,** 295–298.

Gunduz M, Ouchida M, Fukushima K, Hanafusa H, Etani T, Nishioka S, Nishizaki K and Shimizu K. (2000). *Cancer Res.,* **60,** 3143–3146.

Hinds PW and Weinberg RA. (1994). *Curr. Opin. Genet. Dev.,* **4,** 135–141.

Hurlstone AFL, Reid G, Reeves JR, Fraser J, Strathdee G, Rahilly M, Parkinson EK and Black DM. (1999). *Oncogene,* **18,** 1881–1890.

Knudson AG. (1993). *Proc. Natl. Acad. Sci. USA,* **90,** 10914–10921.

Kohno T, Takakura S, Yamada T, Okamoto A, Tanaka T and Yokota J. (1999). *Cancer Res.,* **59,** 4170–4174.

Kukita A, Kukita T, Maeda H, Ouchida M, Yatsuki H and Kohashi O. (1999). *Blood,* **94,** 1987–1997.

Latil A, Cussenot O, Fournier G, Baron JC and Lidereau R. (1995). *Clin. Cancer Res.,* **1,** 1385–1389.

Lin JC, Scherer SW, Tougas L, Traverso G, Tsui LC, Andrulis IL, Jothy S and Park M. (1996). *Oncogene,* **13,** 2001–2008.

Loewith R, Meijer M, Lees-Miller S, Riabowol K and Young D. (2000). *Mol. Cell. Biol.,* **20,** 3807–3816.

Nagashima M, Shiseki M, Miura K, Hagiwara K, Linke SP, Pedeux R, Wang XW, Yokota J, Riabowol K and Harris CC. (2001). *Proc. Natl. Acad. Sci. USA,* **98,** 9671–9676.

Ogata T, Ayusawa D, Namba M, Takahashi E, Oshimura M and Oishi M. (1993). *Mol. Cell. Biol.,* **13,** 6036–6043.

Shimada Y, Saito A, Suzuki M, Takahashi E and Horie M. (1998). *Cytogenet. Cell Genet.,* **83,** 232–235.

Shridhar V, Sun QC, Miller OJ, Kalemkerian GP, Petros J and Smith DI. (1997). *Oncogene,* **15,** 2727–2733.

Skowyra D, Zeremski M, Neznanov N, Li M, Choi Y, Uesugi M, Hauser CA, Gu W, Gudkov AV and Qin J. (2001). *J. Biol. Chem.,* **276,** 8734–8739.

Takahashi S, Shan AL, Ritland SR, Delacey KA, Bostwick DG, Lieber MM, Thibodeau SN and Jenkins RB. (1995). *Cancer Res.,* **55,** 4114–4119.

Tanino M, Matsuo M, Uenaka A, Tsukuda K, Ouchida M, Nakayama E and Shimizu K. (1999). *Mol. Carcinog.,* **26,** 286–297.

Tatarelli C, Linnenbach A, Mimori K and Croce CM. (2000). *Genomics,* **68,** 1–12.

Toyama T, Iwase H, Watson P, Muzik H, Saettler E, Magliocco A, DiFrancesco L, Forsyth P, Garkavtsev I, Kobayashi S and Riabowol K. (1999). *Oncogene,* **18,** 5187–5193.

Wang XL, Uzawa K, Miyakawa A, Shiiba M, Watanabe T, Sato T, Yokoe H and Tanizawa H. (1998). *Int. J. Cancer,* **75,** 671–674.

Wary KK, Mainiero F, Isakoff SJ, Marcantonio EE and Giancotti FG. (1996). *Cell,* **87,** 733–743.

Zenklusen JC, Thompson JC, Klein-Szanto AJP and Conti CJ. (1995). *Cancer Res.,* **55,** 1347–1350.

Zenklusen JC, Oshimura M, Barrett JC and Conti CJ. (1994). *Oncogene,* **9,** 2817–2825.

Zenklusen JC, Hodges LC, Lacava M, Green ED and Conti CJ. (2000). *Oncogene,* **19,** 1729–1733.

Zenklusen JC, Conti CJ and Green ED. (2001). *Nat. Genet.,* **27,** 392–398.

Zeremski M, Hill JE, Kwek SS, Grigorian IA, Gurova KV, Garkavtsev IV, Diatchenko L, Koonin EV and Gudkov AV. (1999). *J. Biol. Chem.,* **274,** 32172–32181.

Zhang JS, Nelson M, Mciver B, Hay ID, Goellner JR, Grant CS, Eberhardt NL and Smith DI. (1998). *Oncogene,* **17,** 789–793.